Research Article | Vol. 24, No. 25 | 12 Dec 2016 | OPTICS EXPRESS 28915

Optics EXPRESS

110-mJ 225-fs cryogenically cooled Yb:CaF_2 multipass amplifier

E. KAKSIS,[1] G. ALMÁSI,[2,3] J. A. FÜLÖP,[2,4] A. PUGŽLYS,[1,5] A. BALTUŠKA,[1,5] AND G. ANDRIUKAITIS[1,*]

[1]*Photonics Institute Vienna University of Technology, Gusshausstrasse 27-387, A-1040 Vienna, Austria*
[2]*MTA-PTE High-Field Terahertz Research Group, Ifjúság ú. 6, H-7624 Pécs, Hungary*
[3]*Institute of Physics and Szentágothai Research Centre, University of Pécs, Ifjúság ú. 6, H-7624 Pécs, Hungary*
[4]*ELI-ALPS, ELI-Hu Nkft., Dugonics Tér 13, H-6720 Szeged, Hungary*
[5]*Center for Physical Sciences & Technology, Savanoriu Ave. 231 LT-02300 Vilnius, Lithuania*
[*]*giedrius.andriukaitis@tuwien.ac.at*

Abstract: We report on a diode-pumped cryogenically cooled bulk Yb:CaF_2 12-pass amplifier delivering 110-mJ, 1030-nm pulses at a 50-Hz repetition rate. The pulses have a spectral bandwidth of 13 nm and are compressed to 225 fs pulse duration in a double reflection grating based compressor having a transmission efficiency of >90%. The measured output beam quality is M^2<1.1. A key feature of the amplifier design is the 4f relay imaging onto the gain medium with progressive beam magnification for the mitigation of the spatial gain narrowing effect. The number of passes in the amplifier is scalable by increasing the size of imaging mirrors. In order to prevent accumulation of nonlinear phase due to self-phase modulation in air, the amplifier is enclosed into a low-vacuum case.

OCIS codes: (140.3280) Laser amplifiers; (140.7090) Ultrafast lasers; (140.3615) Lasers, ytterbium.

References and links

1. J. Zhu, W. Ling, X. Zhong, Z. Wang, and Z. Wei, "High energy picosecond optical parametric amplifier pumped by the second harmonic of a two-stage Ti:sapphire laser," IEEE J. Quantum Electron. **48**(10), 1300–1304 (2012).
2. T. Fuji and T. Suzuki, "Generation of sub-two-cycle mid-infrared pulses by four-wave mixing through filamentation in air," Opt. Lett. **32**(22), 3330–3332 (2007).
3. S.-W. Huang, E. Granados, W. R. Huang, K.-H. Hong, L. E. Zapata, and F. X. Kärtner, "High conversion efficiency, high energy terahertz pulses by optical rectification in cryogenically cooled lithium niobate," Opt. Lett. **38**(5), 796–798 (2013).
4. M. C. Hoffmann and J. A. Fülöp, "Intense ultrashort terahertz pulses: generation and applications," J. Phys. D **44**(8), 083001 (2011).
5. J. A. Fülöp, Z. Ollmann, C. Lombosi, C. Skrobol, S. Klingebiel, L. Pálfalvi, F. Krausz, S. Karsch, and J. Hebling, "Efficient generation of THz pulses with 0.4 mJ energy," Opt. Express **22**(17), 20155–20163 (2014).
6. C. Vicario, A. V. Ovchinnikov, S. I. Ashitkov, M. B. Agranat, V. E. Fortov, and C. P. Hauri, "Generation of 0.9-mJ THz pulses in DSTMS pumped by a Cr:Mg_2SiO_4 laser," Opt. Lett. **39**(23), 6632–6635 (2014).
7. J. A. Fülöp, G. Polónyi, B. Monoszlai, G. Andriukaitis, T. Balciunas, A. Pugzlys, G. Arthur, A. Baltuska, and J. Hebling, "Highly efficient scalable monolithic semiconductor terahertz pulse source," Optica **3**(10), 1075–1078 (2016).
8. K. Y. Kim, J. H. Glownia, A. J. Taylor, and G. Rodriguez, "Terahertz emission from ultrafast ionizing air in symmetry-broken laser fields," Opt. Express **15**(8), 4577–4584 (2007).
9. J. J. Macklin, J. D. Kmetec, and C. L. Gordon 3rd, "High-order harmonic generation using intense femtosecond pulses," Phys. Rev. Lett. **70**(6), 766–769 (1993).
10. G. Korn, A. Thoss, H. Stiel, U. Vogt, M. Richardson, T. Elsaesser, and M. Faubel, "Ultrashort 1-kHz laser plasma hard x-ray source," Opt. Lett. **27**(10), 866–868 (2002).
11. J. A. Fülöp, L. Pálfalvi, M. C. Hoffmann, and J. Hebling, "Towards generation of mJ-level ultrashort THz pulses by optical rectification," Opt. Express **19**(16), 15090–15097 (2011).
12. T. Kapfrath, K. Tanaka, and K. A. Nelson, "Resonant and nonresonant control over matter and light by intense terahertz transients," Nat. Photonics **7**(9), 680–690 (2013).
13. K. Kovács, E. Balogh, J. Hebling, V. Toşa, and K. Varjú, "Quasi-phase-matching high-harmonic radiation using chirped THz pulses," Phys. Rev. Lett. **108**(19), 193903 (2012).
14. J. Hebling, J. A. Fülöp, M. Mechler, L. Pálfalvi, C. Tőke, and G. Almási, "Optical manipulation of relativistic electron beams using THz pulses," arXiv:1109.6852 (2011).
15. L. Pálfalvi, J. A. Fülöp, G. Tóth, and J. Hebling, "Evanescent-wave proton postaccelerator driven by intense THz pulse," Phys. Rev. Spec. Top. Accel. Beams **17**(3), 031301 (2014).

#278604 http://dx.doi.org/10.1364/OE.24.028915
Journal © 2016 Received 12 Oct 2016; revised 27 Nov 2016; accepted 28 Nov 2016; published 6 Dec 2016

Optics EXPRESS

16. E. A. Nanni, W. R. Huang, K.-H. Hong, K. Ravi, A. Fallahi, G. Moriena, R. J. D. Miller, and F. X. Kärtner, "Terahertz-driven linear electron acceleration," Nat. Commun. **6**, 8486 (2015).
17. A. Sharma, Z. Tibai, and J. Hebling, "Intense tera-hertz laser driven proton acceleration in plasmas," Phys. Plasmas **23**(6), 063111 (2016).
18. V. Shumakova, P. Malevich, S. Ališauskas, A. Voronin, A. M. Zheltikov, D. Faccio, D. Kartashov, A. Baltuška, and A. Pugžlys, "Multi-millijoule few-cycle mid-infrared pulses through nonlinear self-compression in bulk," Nat. Commun. **7**, 12877 (2016).
19. T. Popmintchev, M.-C. Chen, D. Popmintchev, P. Arpin, S. Brown, S. Ališauskas, G. Andriukaitis, T. Balčiunas, O. D. Mücke, A. Pugžlys, A. Baltuška, B. Shim, S. E. Schrauth, A. Gaeta, C. Hernández-García, L. Plaja, A. Becker, A. Jaron-Becker, M. M. Murnane, and H. C. Kapteyn, "Bright coherent ultrahigh harmonics in the keV x-ray regime from mid-infrared femtosecond lasers," Science **336**(6086), 1287–1291 (2012).
20. J. Weisshaupt, V. Juvé, M. Holtz, S. A. Ku, M. Woerner, T. Elsaesser, S. Ališauskas, A. Pugžlys, and A. Baltuška, "High-brightness table-top hard X-ray source driven by sub-100-femtosecond mid-infrared pulses," Nat. Photonics **8**(12), 927–930 (2014).
21. D. Kartashov, S. Ališauskas, G. Andriukaitis, A. Pugžlys, M. Schneider, A. Zheltikov, S. L. Chin and A. Baltuška, "Free-space nitrogen gas laser driven by a femtosecond filament," Phys. Rev. A **86**(3), 033831 (2012).
22. A. V. Mitrofanov, A. A. Voronin, D. A. Sidorov-Biryukov, A. Pugžlys, E. A. Stepanov, G. Andriukaitis, T. Flöry, S. Ališauskas, A. B. Fedotov, A. Baltuška, and A. M. Zheltikov, "Mid-infrared laser filaments in the atmosphere," Sci. Rep. **5**, 8368 (2015).
23. M. Siebold, S. Bock, U. Schramm, B. Xu, J. L. Doualan, P. Camy, and R. Moncorgé, "Yb:CaF_2 - a new old laser crystal," Appl. Phys. B **97**(2), 327–338 (2009).
24. A. Pugžlys, G. Andriukaitis, D. Sidorov, A. Irshad, A. Baltuška, W. J. Lai, P. B. Phua, L. Su, J. Xu, H. Li, R. Li, S. Ališauskas, A. Marcinkevičius, M. E. Fermann, L. Giniūnas, and R. Danielius, "Spectroscopy and lasing of cryogenically cooled Yb,Na:CaF_2," Appl. Phys. B **97**(2), 339–350 (2009).
25. A. Kessler, M. Hornung, S. Keppler, F. Schorcht, M. Hellwing, H. Liebetrau, J. Körner, A. Sävert, M. Siebold, M. Schnepp, J. Hein, and M. C. Kaluza, "16.6 J chirped femtosecond laser pulses from a diode-pumped Yb:CaF_2 amplifier," Opt. Lett. **39**(6), 1333–1336 (2014).
26. F. Friebel, S. Ricaud, A. Pellegrina, M. Hanna, E. Mottay, P. Camy, J. L. Doualan, R. Moncorgé, P. Georges, F. Druon, and D. N. Papadopoulos, "High energy and broadband Yb:CaF_2 multipass amplifier using passive coherent combining," in *The Conference on Lasers and Electro-Optics 2013*, paper CA_10_4 (2013).
27. M. Siebold, M. Hornung, R. Boedefeld, S. Podleska, S. Klingebiel, C. Wandt, F. Krausz, S. Karsch, R. Uecker, A. Jochmann, J. Hein, and M. C. Kaluza, "Terawatt diode-pumped Yb:CaF2 laser," Opt. Lett. **33**(23), 2770–2772 (2008).
28. A. Pugžlys, G. Andriukaitis, A. Baltuška, L. Su, J. Xu, H. Li, R. Li, W. J. Lai, P. B. Phua, A. Marcinkevičius, M. E. Fermann, L. Giniūnas, R. Danielius, and S. Ališauskas, "Multi-mJ, 200-fs, cw-pumped, cryogenically cooled, Yb,Na:CaF_2 amplifier," Opt. Lett. **34**(13), 2075–2077 (2009).
29. R. L. Fork, F. A. Beisser, and D. K. Fork, "Multipass optical amplifier using a double confocal resonator geometry," Rev. Phys. Appl. (Paris) **22**(12), 1665–1671 (1987).
30. A. M. Scott, G. Cook, and A. P. G. Davies, "Efficient high-gain laser amplification from a low-gain amplifier by use of self-imaging multipass geometry," Appl. Opt. **40**(15), 2461–2467 (2001).

1. Introduction

Ultrafast strong-field science, a rapidly expanding research field, steadily demands higher peak and average power lasers for pumping secondary radiation sources based on non-linear frequency conversion, such as (i) parametric amplifiers based on $\chi^{<2>}$ and $\chi^{<3>}$ interactions [1,2]; (ii) powerful THz radiation sources relying on optical rectification [3–7] and generation of laser plasma microcurrents [8]; (iii) coherent soft EUV/X-ray generation via higher-order harmonic generation [9]; and (iv) incoherent hard X-ray radiation emerging from K_α and K_β transitions and bremsstrahlung in strongly excited solid-state targets [10].

Recently highly efficient generation of intense THz pulses with energies exceeding 1 mJ was predicted in the low-frequency region of THz spectrum (<1 THz) by optical rectification of 100-mJ-class laser pulses with optimally chosen pulse duration in the sub-ps region [11]. Besides enabling cutting-edge applications, like investigation and control over material properties and their dynamics under the influence of extremely high quasi-static fields [12], or THz-assisted attosecond pulse generation [13], such intense THz pulses are ideally suited for charged-particle manipulation [14] and acceleration [15–17]. Combining efficient diode-pumped solid-state (DPSS) sub-ps pump lasers with novel THz generation techniques and laser-ion acceleration may lead to the realization of compact and versatile ion sources suitable for medical applications [15,17]. Therefore, the development of short-pulse, high-energy pump lasers is highly demanded for novel techniques of THz pulse generation and application.

Optics EXPRESS

Furthermore, high-energy, short-pulse near-IR lasers can serve as a pump for mid-IR optical parametric amplifiers (OPAs). Mid-IR pulses with high intensity, boosted by self-compression in transparent dielectrics [18], are very promising drivers for higher-order harmonic generation, because they allow reaching (multi-)keV energies of coherent EUV/X-ray photons [19]. Moreover, high-energy mid-IR pulses find applications in incoherent X-ray generation [20] and in the field of laser filamentation [21,22]. Drivers of high-energy mid-IR OPAs need to generate both high energy and short duration pulses. The latter is necessary for efficient generation of white light continuum that is used for seeding of ultrashort pulse OPAs.

Among Yb-doped host materials, Yb:CaF_2 is a very attractive laser crystal for high-energy ultrashort pulse amplification. It supports amplification bandwidth of >20 nm FWHM in the multi-mJ pulse energy range [23] and sub-200 fs pulse duration. Yb:CaF_2 has high thermal conductivity, low nonlinear refractive index and long radiation lifetime. The disadvantage of this gain medium is relatively low absorption and emission cross-sections at room temperature (namely, $0.54 \cdot 10^{-20}$ cm^2 and $0.17 \cdot 10^{-20}$ cm^2, correspondingly [23]). Application of cryogenic cooling helps increasing the emission and absorption cross/sections by a factor of 3 [23,24] while preserving sufficient gain bandwidth for amplification of 200-fs pulses. Moreover, cryogenic cooling transforms the room-temperature quasi 3-level system of Yb:CaF_2 into a 4-level system, which improves overall efficiency.

Over the past decade, much effort was invested in the development of both room temperature and cryogenically cooled Yb-doped DPSS amplifiers. A number of regenerative and multipass Yb:CaF_2 amplifier designs have been reported with the parameters peaking at 16.6 J pulse energy at sub-Hz repetition rate [25] and 160 mJ pulse energy at 20 Hz repetition rate [26] in the case of uncompressed ns pulses and reaching 420 mJ energy for compressed femtosecond pulses at 1 Hz repetition rate [27].

In this paper we report on the generation of 110-mJ 225-fs pulses at a repetition rate of 50 Hz, which was achieved in a multipass amplifier (MPA) scheme with cryogenically cooled Yb:CaF_2 as a gain medium.

2. Description of the system

2.1 Pump schematics

The MPA is pumped with the pulsed laser diode (LD) array by Lastronics GmbH, which delivers 2 J pulses at a repetition rate tunable up to 100 Hz. The pump pulse duration of 2 ms matches the radiation lifetime of the gain medium and corresponds to 20% duty cycle when the pump diode operates at 100 Hz and corresponds to the pump peak power of 1 kW. The LD module is not wavelength stabilized, therefore the pump spectrum experiences red-shift with the increase of LD current and/or average optical output power. Because of this temperature-related red shift, at the maximum repetition rate the pump spectrum moves out of the zero phonon line (ZPL) of the Yb:CaF_2 laser crystal reducing pump absorption. In order to preserve optimal pumping efficiency, the repetition rate of the pump module in this work was set to 50 Hz, which leads to a lower thermal load on the LD array at higher current values such that the LD emission wavelength suitably overlaps with the ZPL of Yb:CaF_2.

The layout of the pumping system is presented in Fig. 1. The pump beam from the LD has a nearly-square cross-section, as shown in the left inset to Fig. 1. In order to improve the spatial overlap of the pump and seed beams, the pump beam is reshaped to have round profile with a quasi-supergaussian transversal intensity profile (Fig. 1, right inset).

Optics EXPRESS

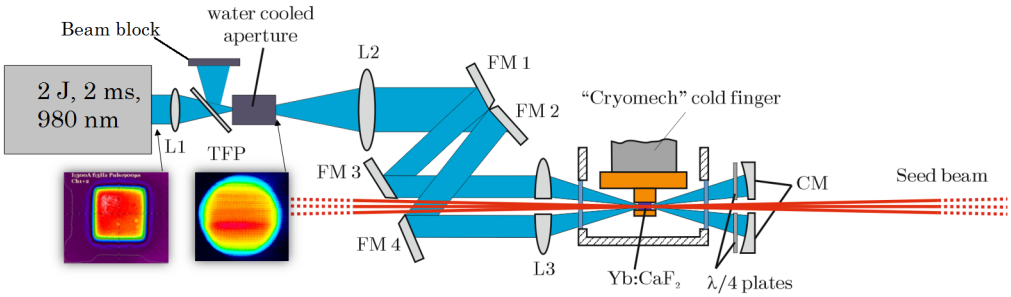

Fig. 1. Layout of pumping system; L1, L2 and L3 - lenses; FM1-4 – folding mirrors; CM – curved mirrors; TFP – thin film polarizer; in the left down corner pump beam profiles before and after the aperture are shown (for details see text).

The reshaping is realized by focusing the pump beam with the lens L1 into a circular water-cooled aperture, which blocks about 30% of power concentrated mainly in the corners of the square-shaped pump beam. In addition to the improved overlap of pump and seed beams, the reshaping reduces thermal load on the amplifier crystal.

After the spatial filtering on the aperture, the pump beam is collimated with the lens L2 and focused by the lens L3 into the laser crystal which results in a pump spot diameter of 2.2 mm. Since broadband dielectric coatings have low damage threshold, we aimed to avoid usage of dichroic mirrors, which are commonly employed for injection of the pump radiation into the gain medium. Instead of using dichroic mirrors, we split the pump into two beams by two pairs of flat silver mirrors FM1,2 and FM3,4 correspondingly. The lens L3 is cut in two, with two halves spatially separated to form an opening through which the amplified 1030-nm pulses pass. The 2%-Yb-doped, 7-mm-long CaF_2 crystal (Hellma Materials) is uncoated and oriented at a Brewster's angle. Single-pass pump absorption in absence of seeded amplification is about 70%. The residual transmitted pump light from the LD is reimaged in a 2*f*-2*f* configuration with a curved mirror CM. Similarly to the lens L3, the pump mirror CM is divided in two separated halves. Including the return pass through the laser crystal, about 90% of the pump light is absorbed in the gain medium. In order to prevent the 10% of unabsorbed pump light from returning to the LD, the polarization of the returning residual pump beam is rotated by λ/4 wave plates installed in front of each segment of the mirror CM. A thin-film polarizer (TFP) in front of the LD transmits the outgoing pump beam and rejects the incoming residual orthogonally polarized light.

2.2 Schematics of the multipass amplifier

A layout of Yb:CaF_2multipass amplifier is depicted in Fig. 2. Since Yb:CaF_2 in general is a low gain medium [24], in order to increase a single pass gain 2-% doped 7-mm long Yb:CaF2 crystal in the amplifier is cryogenically cooled to 35 K temperature by a close loop cryo-refrigerator (Cryomech PT90) having 48 W cooling capacity at 50 K temperature. At full pump load of 200 W the temperature of the crystal rises to 55 K. Yb:CaF2 crystal was aligned in such a way that the laser beam was propagating along [111] direction. The amplifier is seeded by the output of a cryogenically cooled Yb:CaF_2 chirped pulse regenerative amplifier [28], which generates 12 mJ, 500 ps pulses with the spectrum supporting sub-200 fs pulse duration.

The input beam is relay-imaged by the curved mirrors CM1 and CM2 onto the laser crystal, whereupon another pair of curved mirrors, CM3 and CM4, reimages the beam onto the flat mirror FM1. Successively, the optical system reimages the beam from FM1 to the laser crystal, and from the laser crystal onto FM2. Without destroying the overlap of the amplifier beams in the laser crystal, the directions of individual passes are fanned out with small angular pitches by adjusting the tilt of the flat mirror FM2 placed in the image plane. The number of passes is limited to 12 by the 2-inch aperture of the curved mirrors CM1-4. The input beam is injected into the amplifier below the central plane of the mirror CM1 (Fig.

Optics EXPRESS

2, inset), while the output beam is ejected above the central plane of CM1, and is picked off by a prism-shaped dielectric coated mirror.

Note that the seed beam propagates through the gain medium collimated, while the foci are located between the curved mirrors CM1 and CM2, and CM3 and CM4 correspondingly. This makes the design more compact, as compared to the systems with laser crystal placed in the focal plane of curved mirrors [29], because it does not require mirrors with long focal distances that would be required to provide adequately large focal spot diameters in the gain medium.

The use of the self-imaging arrangement [30] described above allows controlling the input beam diameter on the crystal through all the passes. The size of the input beam injected into the MPA is adjusted with the lens telescope shown in Fig. 2. An appropriate spot diameter is determined by the damage threshold of the mirror coatings estimated at 7 J/cm^2. Accordingly, the input beam diameter was set to 2.2 mm at the 1/e^2 level, which corresponds to ~3 J/cm^2 energy fluence at 110 mJ pulse energy.

Self-imaging of the laser beam in the amplifier is perturbed by thermal lens and spatial gain narrowing in the laser crystal. The induced thermal lens affects the image relay distance and is compensated through longitudinal position adjustment of the mirror CM1. Because of the thermal lens, the amplifier is operated at a certain fixed pump power. Spatial gain narrowing, which takes place during amplification, leads to a progressive decrease of the beam diameter and rapid increase of energy fluence, thus also increasing the risk of optical damage. To balance out the spatial gain narrowing, an additional D-shaped mirror DM with the radius of curvature slightly smaller than that of CM4 is installed as it is shown in Fig. 2.

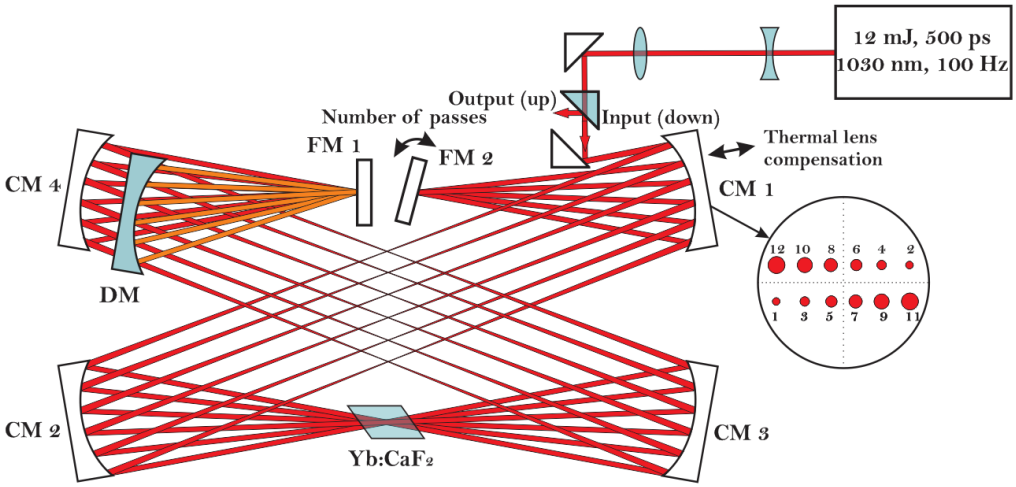

Fig. 2. Schematics of the multipass amplifier. CM1-4 – curved mirrors with the radii of curvature of 200 cm; FM1, 2 – flat mirrors; DM – D-shaped mirror with the radius of curvature of 184 cm; in the circle the arrangement and relative sizes of the beams at different passes (indicated by numbers) on the curved mirror CM1 when gain is switched off, is illustrated.

The mirror DM, which in pair with CM3 forms a magnifying telescope, intercepts each reflection from the flat mirror FM1 and thus provides progressive expansion of the beam diameter. In absence of amplification, the beam size of the seed beam passed through the MPA progressively increases in steps, as shown schematically in the inset to Fig. 2. In the presence of amplification, the beam size is maintained roughly constant for all the passes as a result of the magnification being counterbalanced by spatial gain narrowing.

Operation of the multipass amplifier on the optical table in an open environment revealed a presence of self-phase modulation (SPM) in air, which leads to an uncontrolled spectral broadening and poor compressibility of amplified pulses, as can be seen in Fig. 3.

Optics EXPRESS

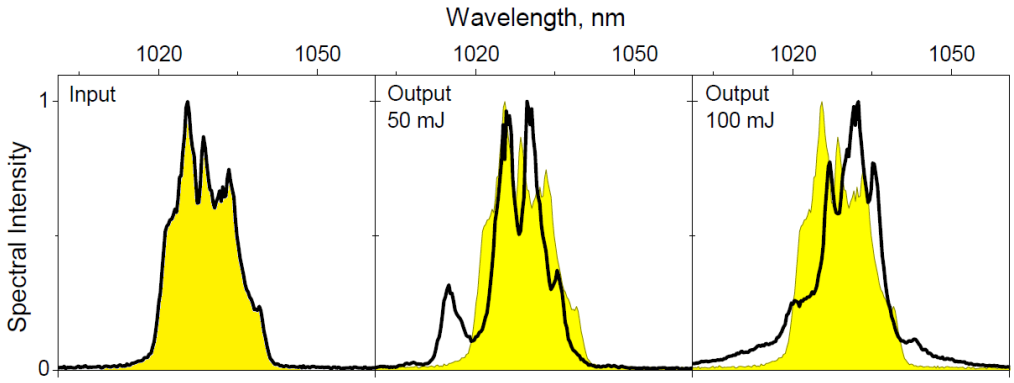

Fig. 3. Influence of SPM in air on the spectrum of the amplified pulse. Left panel: input spectrum. Middle and right panels: output spectra of the MPA at output pulse energies of 50 mJ and 100 mJ, respectively ; by the shadowed area the input spectra are shown.

In order to mitigate SPM, the amplifier was enclosed into a low vacuum case consisting of two aluminum chambers connected by an x-shaped aluminum tubing (see Fig. 4) and capable of sustaining few-mbar pressure. Optical breadboards in the aluminum chambers are decoupled from the chamber walls via flexible hoses, which provides robustness and resistivity against misalignment during chamber evacuation.

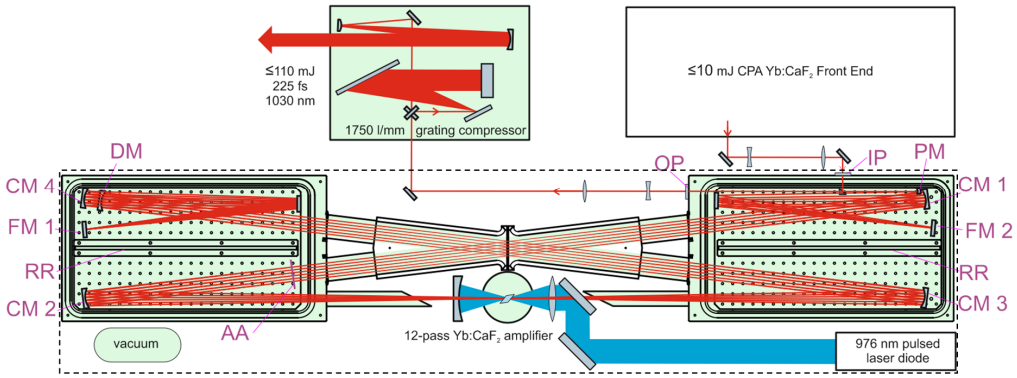

Fig. 4. Top view of the multipass amplifier enclosed in a low-vacuum shell evacuated to the pressure of 1 mbar. IP – input port, OP – output port, PM – pick-off mirror, CM1-4 – curved mirrors, AA - aperture mask, RR – rigidity rib, FM1,2 – flat mirrors, DM – D-shaped mirror. Arrangement of pump is simplified. Detailed pump arrangement is presented in the Fig. 1. Dimensions of the multipass amplifier (marked by a dashed line) are 2.2x0.4 m^2 (LxW).

3. Performance of the multipass amplifier

Because of the thermal drift of the LD wavelength discussed above, the multipass amplifier currently operates at 50 Hz repetition rate and produces up to 120-mJ pulses (Fig. 5(a)) with the spectral bandwidth extending from 1020 nm to 1040 nm (Fig. 6(d)). Absence of the saturation of the output pulse energy confirms that potential further increase of the pulse energy is possible by increasing the number of roundtrips, as the scaling of the average power is possible by scaling up the repetition rate of the system. Currently further increase of the pulse energy is limited by the laser-induced damage of mirror coatings, especially that of CM1 at the final bounce.

The self-imaging arrangement of the amplifier leads to an excellent spatial output beam quality as is confirmed by M^2 measurements, presented in Fig. 5(b). M^2 was determined by recording beam profiles along the focus of a plano-convex $f = 50$ cm fused silica lens. The M^2 values of the output beam are below 1.1 in both the x and y directions. The beam is slightly

Optics EXPRESS

astigmatic which can be either due to the spherical astigmatism of the curved amplifier mirrors and/or astigmatic thermal lens in the slab-shaped laser crystal.

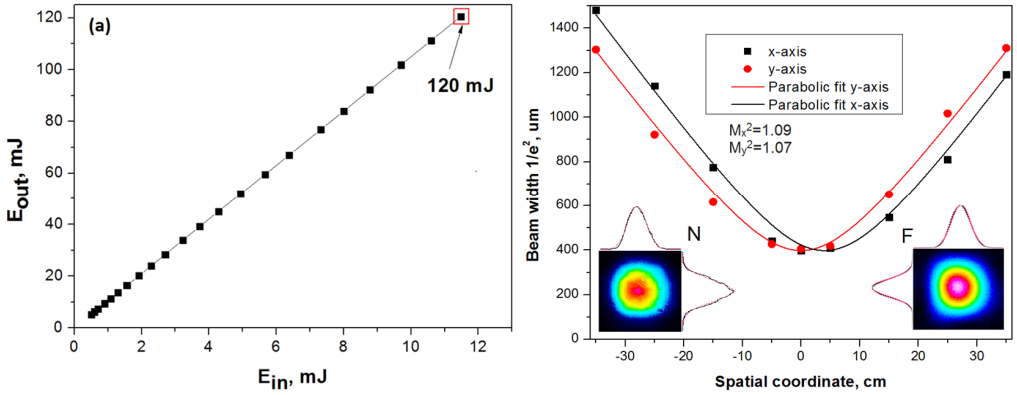

Fig. 5. (a) Dependence of the output energy of the multipass amplifier on the input seed energy; (b) measurement of the M^2 parameter, in the inset near (N) and far (F) field profiles recorded by a beam profiler.

As confirmed by second harmonic generation frequency resolved optical gating (SHG FROG) measurements presented in Fig. 6, the amplified pulses can be compressed to a 225-fs pulse duration.

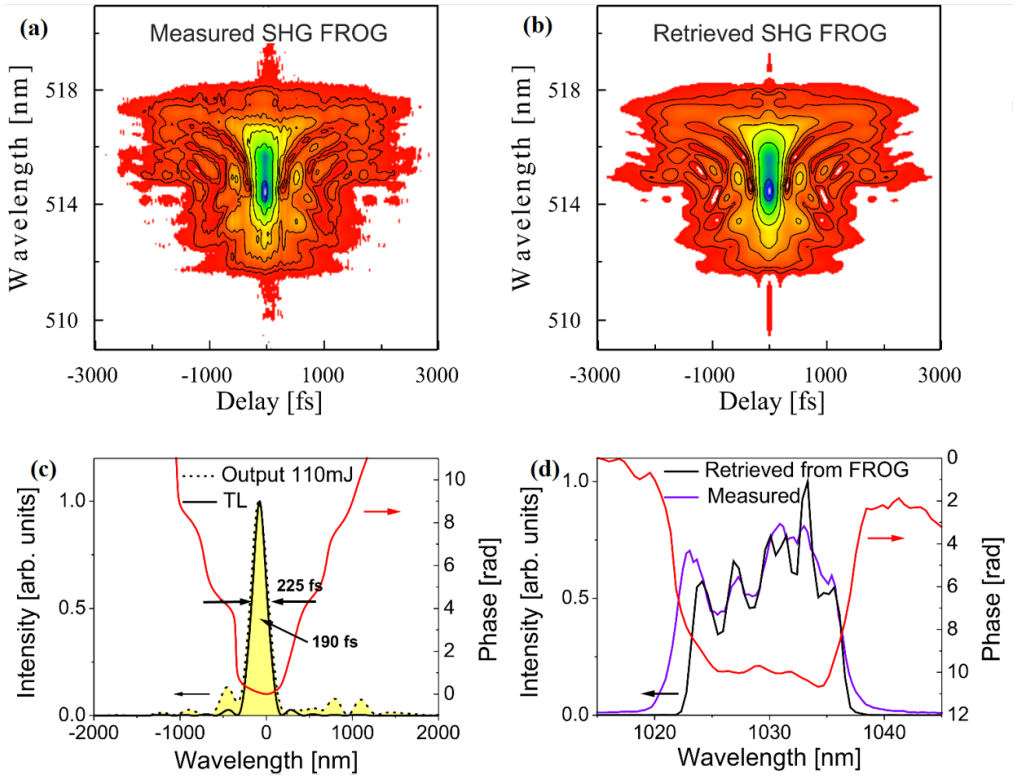

Fig. 6. SHG-FROG measurement of the amplified 110-mJ pulses. (a) Measured SHG-FROG trace; (b) retrieved SHG-FROG trace; (c) Temporal intensity and phase profiles (shaded with yellow – retrieved, solid black line - transform limited); (d) measured and retrieved spectral intensity profile, retrieved spectral phase profile.

Optics EXPRESS

Treacy-type compressors based on a pair of 1750 lines/mm reflective diffraction gratings (Fraunhofer IOF, Jena) were used. Because of the limited grating size, two successive grating pairs were used to cope with the relatively large stretched pulse duration of 500 ps. The first grating pair is in ambient air, and the second pair for final compression is placed in a vacuum chamber filled with He.

Due to the excellent diffraction efficiency of the gratings (~99%) (lithographic reflection gratings, Fraunhofer IOF Jena) and rather good (better than 1:50) polarization contrast of amplified pulses the overall transmission of both compressors exceeded 90%. The Fourier transform limited duration of the amplified pulses is 190 fs (Fig. 6(c)) which suggests that with more careful dispersion management (using similar groove density diffraction gratings for the stretcher and compressor or by implementing in the stretcher or compressor a piezoelectric deformable mirror) sub-200 fs pulses with peak powers exceeding 0.5-TW level can be extracted from the amplifier.

4. Conclusions

In conclusion, we have demonstrated a rather compact and robust Yb:CaF_2 multipass amplifier based on a cryogenically cooled laser crystal and a self-imaging arrangement. The compactness of the amplifier is achieved by employing a 4*f* imaging scheme that permits to propagate a collimated beam through the gain medium. The robustness is achieved by a simple opto-mechanical design that enables straightforward compensation of thermal lens and provides mechanical isolation from a low-vacuum shell enclosing the MPA. In addition, spatial gain narrowing is compensated by an employment of magnifying telescope providing progressive expansion of the beam diameter at each consecutive pass in the amplifier. At 50 Hz the MPA system currently delivers 110-mJ, 225-fs pulses in a high spatial quality beam with $M^2 < 1.1$. With more careful dispersion management, the amplifier is rated to produce sub-200 fs pulses, which would lead to peak powers exceeding 0.5 TW. The absence of gain saturation suggests that wavelength stabilization of the LD should permit a 100-Hz repetition rate and >10 W average power out of the MPA. The developed amplifier has large potential for both direct high-field physics applications and as a driver for secondary mid-IR and THz radiation sources.

Funding

Austrian Science Fund (FWF), SFB NextLite F4903-N23, project P 27491; Hungarian Scientific Research Fund (OTKA), Grant 113083; Hungarian Academy of Sciences (MTA) (János Bolyai Research Scholarship to J. A. Fülöp).

Acknowledgments

The Authors are grateful to Joachim Hein, Friedrich Schiller University Jena, for valuable discussions on Yb:CaF_2.